Letters

Femtosecond Laser Inscribed Sapphire Fiber Bragg Grating for High Temperature and Strain Sensing

Qi Guo, Yong-Sen Yu, Zhong-Ming Zheng, Chao Chen, Peng-Long Wang, Zhen-Nan Tian, Yang Zhao, Xin-Yu Ming, Qi-Dai Chen, Han Yang, and Hong-Bo Sun, *Fellow, IEEE*

***Abstract*—In this letter, a sapphire fiber Bragg grating (SFBG) is fabricated by a femtosecond laser line-by-line scanning method. A third-order fiber Bragg grating is obtained in a single crystal sapphire fiber with a diameter of 60 μm. Compared to the SFBG written by a point-by-point method, the SFBG written by the line-by-line method has a higher reflectivity and grating with about 15% reflectivity is achieved when the track length is about 40 μm. The temperature sensing characteristics of this SFBG from a room temperature to 1600 °C are studied, and the temperature sensitivity of SFBG is 34.96 pm/°C from 1000 °C to 1600 °C. The strain characteristics are also tested at the temperature of 26 °C, 500 °C, 1000 °C, and 1600 °C, and the strain sensitivities are 1.42, 1.42, 1.44, and 1.45 pm/$\mu\varepsilon$, respectively. These characteristics show that this SFBG has potential applications in a harsh environment structural health monitoring.**

***Index Terms*—Sapphire fiber Bragg grating, femtosecond laser, line-by-line scanning, structural health monitoring.**

I. Introduction

THE optic fiber sensors have the advantages of anti-electromagnetic interference and high temperature resistance, which make it possible to replace electronic sensors in extremely harsh environment sensing applications [1]–[3]. Silica-based FBGs have played an important role in fiber grating sensing applications over the past few decades. With the development of grating preparation technology, the application range of FBG has been gradually expanded. The FBGs prepared by ultraviolet laser induced photosensitized refractive fibers are easily thermally erased at high temperature. B.O. Guan *et al.* fabricated type IIa Bragg grating in microfibers by use of the 193 nm excimer laser and proved that it could work stably at 800 °C [4]. In recent years, fs laser processing technology has developed rapidly. The fs laser direct writing is a 3D processing technique with high resolution [5] and the size and direction of the laser processing area can be precisely controlled by the program [6], [7]. This technique pushes up the extreme operating temperature of FBG because a permanent refractive index change in the laser modulation region can be realized by fs laser pulses. The regenerated FBGs can exist stably in the temperature range of 1000 °C [8], but due to the fabrication process, these FBGs are very brittle [9]. Furthermore, limited by the softening point(1330 °C) of quartz crystals and thermal diffusion of the germanium dopant [10], silica-based FBGs cannot work in higher temperature sensing applications, while sapphire fiber has stable chemical properties, high melting point (2053 °C) and good mechanical strength. Therefore, in sensing applications of extremely harsh environments, such as aero-engine, space craft and nuclear reactors, the sensors built by sapphire fiber with these advantages have become a hot research direction in the field of fiber sensing in recent years [11]–[14]. Mihailov *et al.* were the first to prepare an SFBG by phase mask method with a femtosecond laser [15]. Sun *et al.* used phase mask method to prepare an SFBG, obtained higher reflectivity and theoretically analyzed its multimode resonance characteristics [16]. Bartlett *et al.* inscribed SFBGs by phase mask based Talbot interferometry [17]. Wang *et al.* fabricated SFBGs via the point-by-point method by fs laser and characterized its reflection spectrum [18].

However, due to expensive cost and the fixed grating period characteristics, the phase mask technique has difficulties in preparing a variety of FBG arrays with different grating periods. The interferometer method requires a stable platform and accurate cantilever angle. The reflectivity of SFBGs obtained by point-by-point method is relatively low according to current reports. In this letter, an SFBG in 60 um-diameter single crystal sapphire fiber with the track length of 40 um is fabricated by fs laser line-by-line scanning method. This SFBG has stronger refractive index modulation and higher reflectivity compared with SFBG prepared by point-by-point method. In addition, the high

Manuscript received October 18, 2018; revised November 24, 2018; accepted December 14, 2018. Date of publication January 7, 2019; date of current version January 31, 2019. This work was supported in part by the National Key Research and Development Program of China under Grants and National Natural Science Foundation of China (NSFC) under Grants 2017YFB1104300, 91860140, 61590930, 61435005 and 51335008. The review of this letter was arranged by Associate Editor Gwo-Bin Lee. *(Corresponding author: Yong-Sen Yu.)*

Q. Guo, Y.-S. Yu, P.-L. Wang, Z.-N. Tian, Y. Zhao, X.-Y. Ming, Q.-D. Chen, and H. Yang are with the State Key Laboratory of Integrated Optoelectronics, College of Electronic Science and Engineering, Jilin University, Changchun 130012, China (e-mail: yuys@jlu.edu.cn).

Z.-M. Zheng and C. Chen are with the Changchun Institute of Optics, Fine Mechanics and Physics, Chinese Academy of Sciences, Changchun 130033, China.

H.-B. Sun is with the State Key Laboratory of Integrated Optoelectronics, College of Electronic Science and Engineering, Jilin University, Changchun 130012, China, and also with the Department of Precision Instrument, Tsinghua University, Beijing 100084, China.

Digital Object Identifier 10.1109/TNANO.2018.2888536

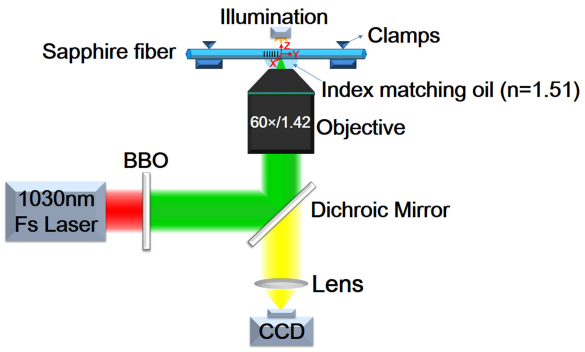

Fig. 1. The schematic diagram of line-by-line scanning method.

temperature and strain sensing characteristics of SFBG have also been studied.

II. Experiments

Fig. 1 shows a schematic diagram of a device for preparing an SFBG by a line-by-line scanning method. The fs laser (Light-Conversion Pharos) provides pulses with an emission wavelength of 1030 nm and pulse width of 290 fs. The repetition rate and pulse energy are 150 Hz and 90 nj. These pulses are frequency doubled in a nonlinear crystal (β-BaB_2O_4) (BBO) to produce pulses with a wavelength of 515 nm [19]. The fs laser pulses are reflected by a dichroic mirror and focused through a high numerical aperture 60× oil immersion objective (Olympus, NA = 1.42) within a sapphire fiber placed on an assembled five-axis processing platform (Aerotech ABL10050L-LN/UPPER and BOCIC MRS100 Series). The phase matching condition of FBG is as follows [20], [21]

$$m\lambda_B = 2n_{eff}\Lambda \tag{1}$$

where m is the order of FBG, λ_B is the wavelength, n_{eff} is the effective refractive index and Λ is the period of the grating. The sapphire fiber has a refractive index of 1.745 at 1550 nm. When $m = 3$ and $\Lambda = 1.332$ μm are selected, a third-order SFBG resonance peak at this wavelength can be obtained.

The SFBG was written in the middle of a 20 cm sapphire fiber with a diameter of 60 μm. The position of the sapphire fiber processed by the fs pulses was observed by a charge coupled device (CCD). The center position of the sapphire fiber was set as the origin (0, 0, 0) of the three-dimensional coordinate. Turn on the laser shutter and scan from the point (20 μm, 0, 0) to the point (-20 μm, 0, 0) along the X-axis. When completing this process, turn off the shutter and scan a grating period along the positive direction of the Y-axis. After scanning a period distance, turn on the shutter and scan from point (-20 μm, 1.332 μm, 0) to point (20 μm, 1.332 μm, 0). Repeat this process until the whole moving distance reaches 2 mm in the positive direction of the Y-axis. The X-axis scanning speed is 0.04 mm/s, and the Y-axis scanning speed is 0.01 mm/s. Low scanning speeds can ensure stable operation of the processing system. Fig. 2 shows that in a 60 μm sapphire fiber, the track length is 40 μm, the track depth is 5.36 μm, and the grating period is 1.332 μm.

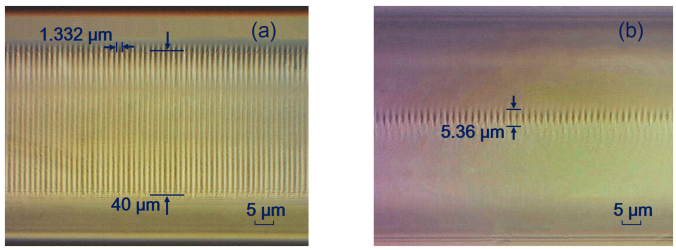

Fig. 2. (a) The top view and (b) side view photomicrographs of fabricated SFBG.

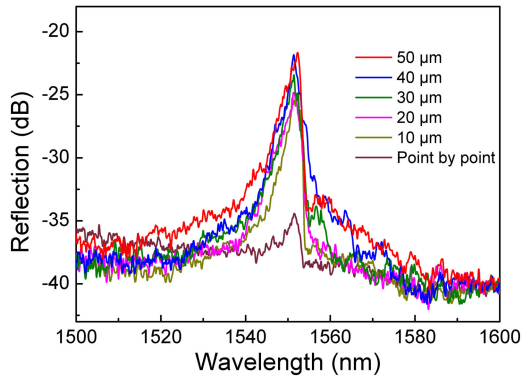

Fig. 3. Spectral comparison of SFBG fabricated by point-by-point method and line-by-line scanning method with different track length.

III. Results and Discussions

In order to compare the SFBG reflectivity fabricated by point-by-point method and line-by-line scanning method with different track length, a grating with a period of 1.332 μm and a length of 2 mm is fabricated by line-by-line scanning method and another grating is fabricated by point-by-point method in a 10 cm-long sapphire fiber. The track length of the line-by-line scanning method is 10 μm, 20 μm, 30 μm, 40 μm, and 50 μm, respectively. Fig. 3 shows a comparison of the SFBG reflectance spectra produced by different processing methods. It is seen that the reflectivity of the fiber grating obtained by the line-by-line scanning method is higher than that of the grating obtained by point-by-point method. At the same time, as the track length increases, the refractive index modulation area increases and the reflection peak broadens. It was found that under the condition of the same processing parameters, when the track length reaches 50 μm, the obtained spectral effect is basically the same as that of the track length of 40 μm. In order to obtain a fiber grating with high reflectivity and mechanical strength, we choose line-by-line scanning method to obtain an SFBG with track length of 40 μm.

The connection between the sapphire fiber and the spectrometer is achieved by fusion with a 62.5/125 μm quartz multimode fiber coupler. The micrograph of the fusion area is shown in the inset of Fig. 4(a). By controlling the discharge current and discharge time of the fiber fusion splicer (Ericsson FSU-975), the quartz fiber is melted and wrap around the sapphire fiber end face and the axial alignment of the two fibers is controlled by high precision moving motors. The discharge current and discharge

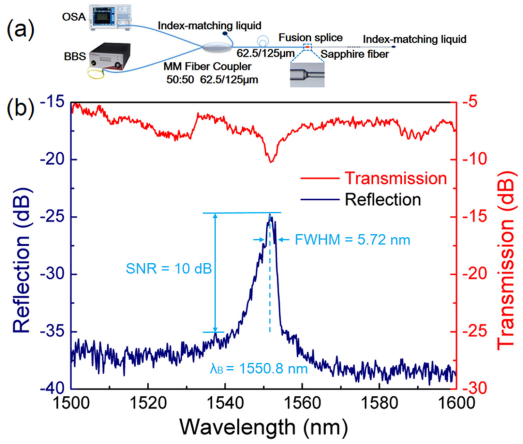

Fig. 4. (a) Schematic diagram of the spectum measurement setup. The illustration shows the welded end face between sapphire fiber and multimode quartz fiber. (b) Reflection and transmission spectrum of SFBG.

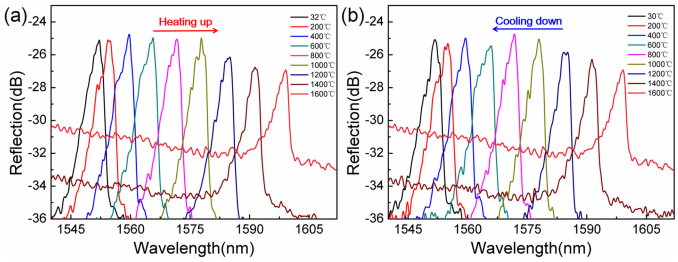

Fig. 5. The reflection spectrum of the SFBGs varies with temperature during the processes of (a) heating and (b) cooling.

time are set to 10 mA and 1.5 s. Before fusion, the sapphire fiber end face is cut smoothly with a fiber cutter to reduce the scattering loss caused by rough end face. This method can achieve rapid fusion of sapphire fiber and quartz fiber, and ensure stable coupling efficiency and mechanical strength [22]. The characterization of the SFBG spectrum is shown in Fig. 4(b). Due to the large diameter of the sapphire fiber mode field, numerous modes are coupled to form a broadband reflection peak. The center wavelength of the reflection spectrum is 1550.8 nm, and the full width at half maximum is 5.72 nm. From the transmission spectrum obtained by polishing the end face of SFBG and testing, the reflectivity is about 15%. The loss in transmission spectrum is mainly due to the coupling loss and the multimode transmission loss of sapphire fiber.

The sapphire fiber is first placed in a customized high temperature furnace with accuracy of ±1 °C and the maximum temperature of 1600 °C measured by a B-type thermocouple. This SFBG is held at 1600 °C for 6 hours and then cooled to room temperature. During the test, the temperature rises from room temperature to 1600 °C and the rate of temperature is set to 10 °C/min. For every 100 °C increment, the temperature is kept constant for 30 minutes and spectrum is recorded by OSA. The cooling process test is the inverse process of the heating process test. The temperature response of SFBG is shown in Fig. 5.

Similar to quartz fiber gratings, the reflection peak of SFBG is apparently red-shifted with the increment of temperature.

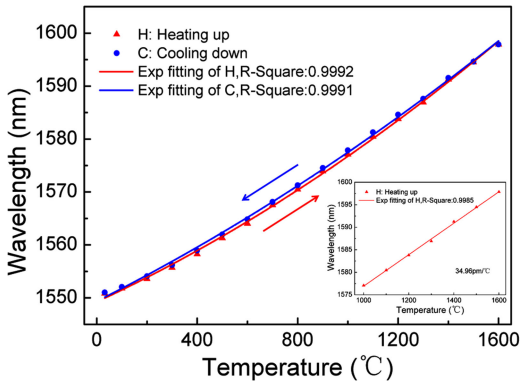

Fig. 6. The relationship between the resonance wavelength of SFBG and temperature. The illustration shows a linear fitting of the resonance wavelength and temperature of SFBG from 1000 °C to 1600 °C.

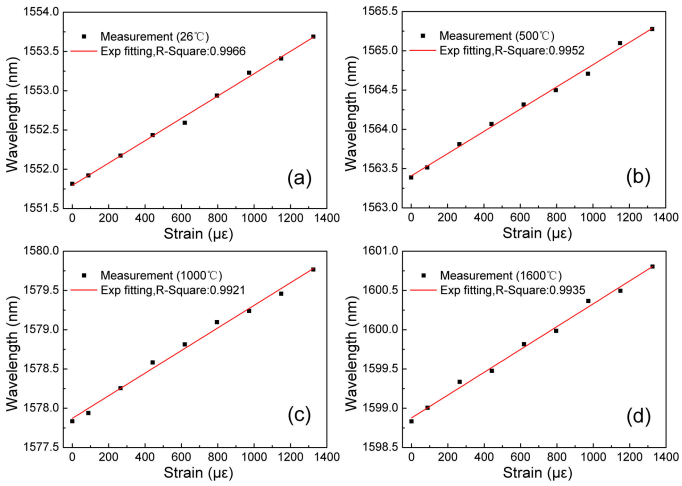

Fig. 7. (a)-(d) The relationship between resonance wavelength and strain of SFBG at different temperature.

When the temperature rises up above 1400 °C, the signal-to-noise ratio (SNR) of the SFBG reflection peak is reduced by the strong background light generated by the black body radiation [23]. Fig. 6 shows the quadratic function fitting curve of the resonance wavelength as a function of temperature. The linear temperature response exhibits a sensitivity of about 34.96 pm/°C from 1000 °C to 1600 °C. The quadratic fitting function is given by

$$\lambda_B = 1549.2366 + 0.02204\mathrm{T} + 5.4625 \times 10^{-6} T^2 \quad (2)$$

The axial strain response of SFBG is tested at room temperature (26 °C), 500 °C, 1000 °C and 1600 °C, respectively. A tension of 0–1.5 N is applied along the axial direction of the fiber by a testing machine (WDW-100). Axial strain can be obtained from the equation $\varepsilon = F/\pi r^2 E$ [24], where F is the axial tension, r is the fiber radius and $E = 400$ GPa is the Young's modulus [25]. Fig. 7 shows the relationship between resonance wavelength and strain at different temperatures. The strain sensitivities are 1.42 pm/$\mu\varepsilon$, 1.42 pm/$\mu\varepsilon$, 1.44 pm/$\mu\varepsilon$ and 1.45 pm/$\mu\varepsilon$, respectively.

The relationship between the variation of SFBG resonance wavelength and the variation of temperature and strain can be obtained by [16], [25]

$$\Delta\lambda_B = \lambda_B(1 - p_e)\Delta\varepsilon + \lambda_B(\alpha_s + \zeta_s)\Delta T \qquad (3)$$

where ΔT and $\Delta\varepsilon$ are the variation of temperature and axial strain, $\alpha_s = 7.15 \times 10^{-6}K^{-1}$ and $\zeta_s = 12.6 \times 10^{-6}K^{-1}$ are the thermal expansion coefficient and the thermo-optic coefficient (at 633 nm) along the c axis of sapphire, $p_e = 0.1277$ is the elastic optic coefficient. The variation of the resonance wavelength is 47.3 nm at $\lambda_B = 1550.8$ nm with no applied strain from 32 °C to 1600 °C, which is consistent with the theoretical calculation of 48.0 nm from Eq. (3). For this SFBG, the calculated strain sensitivities are 1.35 pm/$\mu\varepsilon$, 1.36 pm/$\mu\varepsilon$, 1.38 pm/$\mu\varepsilon$ and 1.39 pm/$\mu\varepsilon$ at 26 °C ($\lambda_B =$ 1550.6 nm), 500 °C ($\lambda_B =$ 1563.4 nm), 1000 °C ($\lambda_B =$ 1577.8 nm) and 1600 °C ($\lambda_B =$ 1598.8 nm), respectively, which match well with the experimental results.

IV. Conclusion

In conclusion, the spectrum of SFBG inscribed in 60 um-diameter sapphire fibers via line-by-line scanning method by fs laser pulses has been characterized and the length of the scanning line covers 66% of the fiber diameter. Experiment results indicate that the Bragg resonance peak performs a higher reflectivity compared with that of SFBG fabricated by point-by-point method and the experimental data of this letter is in accordance with theoretical results. Furthermore, by studying the temperature and strain sensing characteristics of SFBG fabricated by this method, we know that its temperature and strain response is stable at 1600 °C, which illustrates that this SFBG has potential applications in embedded temperature and strain sensing such as the structural health monitoring of aero-engine and space craft.

References

[1] B. Liu *et al.*, "Sapphire-fiber-based distributed high-temperature sensing system," *Opt. Lett.*, vol. 41, no. 18, pp. 4405–4408, 2016.

[2] A. Yan, R. Chen, M. Zaghloul, Z. L. Poole, P. Ohodnicki, and K. P. Chen, "Sapphire fiber optical hydrogen sensors for high-temperature environments," *IEEE Photon. Technol. Lett.*, vol. 28, no. 1, pp. 47–50, Jan. 2015.

[3] S. J. Mihailov, "Fiber Bragg grating sensors for harsh environments," *Sensors*, vol. 12, no. 2, pp. 1898–1918, 2012.

[4] R. Yang *et al.*, "Type IIa Bragg gratings formed in microfibers," *Opt. Lett.*, vol. 40, no. 16, pp. 3802–3805, 2015.

[5] L. Wang *et al.*, "Plasmonic nano-printing: Large-area nanoscale energy deposition for efficient surface texturing," *Light Sci. Appl.*, vol. 6, no. 12, 2017, Art. no. e17112.

[6] B. Poumellec, M. Lancry, R. Desmarchelier, E. Hervé, and B. Bourguignon, "Parity violation in chiral structure creation under femtosecond laser irradiation in silica glass?," *Light Sci. Appl.*, vol. 5, no. 11, 2017, Art. no. e16178.

[7] J. Ni *et al.*, "Three-dimensional chiral microstructures fabricated by structured optical vortices in isotropic material," *Light Sci. Appl.*, vol. 6, no. 7, 2017, Art. no. e17011.

[8] J. He *et al.*, "Negative-index gratings formed by femtosecond laser overexposure and thermal regeneration," *Scientific Reports*, vol. 6, no. 10, p. 23379, 2016.

[9] T. Habisreuther, T. Elsmann, A. Graf, and M. A. Schmidt, "High-temperature strain sensing using sapphire fibers with inscribed first-order Bragg gratings," *IEEE Photon. J.*, vol. 8, no. 3, Jun. 2016, Art. no. 6802608.

[10] Y. Zhu, Z. Huang, F. Shen, and A. Wang, "Sapphire-fiber-based white-light interferometric sensor for high-temperature measurements," *Opt. Lett.*, vol. 30, no. 7, pp. 711–713, 2005.

[11] S. Yang, D. Homa, G. Pickrell, and A. Wang, "Fiber Bragg grating fabricated in micro-single-crystal sapphire fiber," *Opt. Lett.*, vol. 43, no. 1, pp. 62–65, 2018.

[12] H. Xiao, J. Deng, G. Pickrell, and R. G. May, "Single-crystal sapphire fiber-based strain sensor for high-temperature applications," *J. Lightw. Technol.*, vol. 21, no. 10, pp. 2276–2283, 2003.

[13] A. Wang, B. Dong, E. Lally, J. Wang, J. Gong, and M. Han, "Multiplexed high temperature sensing with sapphire fiber air gap-based extrinsic Fabry–Perot interferometers," *Opt. Lett.*, vol. 35, no. 5, pp. 619–621, 2010.

[14] H. Chen, F. Tian, J. Kanka, and H. Du, "A scalable pathway to nanostructured sapphire optical fiber for evanescent-field sensing and beyond," *Appl. Phys. Lett.*, vol. 106, no. 11, pp. 8–61, 2015.

[15] D. Grobnic, S. J. Mihailov, C. W. Smelser, and H. Ding, "Sapphire fiber Bragg grating sensor made using femtosecond laser radiation for ultrahigh temperature applications," *IEEE Photon. Technol. Lett.*, vol. 16, no. 11, pp. 2505–2507, Nov. 2004.

[16] C. Chen *et al.*, "Femtosecond laser-inscribed high-order Bragg gratings in large-diameter sapphire fibers for high-temperature and strain sensing," *J. Lightw. Technol.*, vol. 36, no. 16, pp. 3302–3308, Aug. 2018.

[17] T. Elsmann, T. Habisreuther, A. Graf, M. Rothhardt, and H. Bartelt, "Inscription of first-order sapphire Bragg gratings using 400 nm femtosecond laser radiation," *Opt. Express*, vol. 21, no. 4, pp. 4591–4597, 2013.

[18] S. Yang, D. Hu, and A. Wang, "Point-by-point fabrication and characterization of sapphire fiber Bragg gratings," *Opt. Lett.*, vol. 42, no. 20, pp. 4219–4222, 2017.

[19] A. Vorobyev, C. Guo, and R. Fang, "Direct visualization of the complete evolution of femtosecond laser-induced surface structural dynamics of metals," *Light Sci. Appl.*, vol. 6, no. 3, 2017, Art. no. e16256.

[20] C. Chen *et al.*, "Reflective optical fiber sensors based on tilted fiber Bragg gratings fabricated with femtosecond laser," *J. Lightw. Technol.*, vol. 31, no. 3, pp. 455–460, 2013.

[21] D. N. Nikogosyan, "REVIEW ARTICLE: Multi-photon high-excitation-energy approach to fibre grating inscription," *Meas. Sci. Technol.*, vol. 18, no. 1, pp. 1–29, 2007.

[22] Y. Zhu and A. Wang, "Surface-mount sapphire interferometric temperature sensor," *Appl. Opt.*, vol. 45, no. 24, pp. 6071–6076, 2006.

[23] C. R. Liao and D. N. Wang, "Review of femtosecond laser fabricated fiber Bragg gratings for high temperature sensing," *Photon. Sens.*, vol. 3, no. 2, pp. 97–101, 2013.

[24] Z. M. Zheng, Y. S. Yu, X. Y. Zhang, Q. Guo, and H. B. Sun, "Femtosecond laser inscribed small-period long-period fiber gratings with dual-parameter sensing," *IEEE Sensors J.*, vol. 18, no. 3, pp. 1100–1103, Feb. 2018.

[25] S. J. Mihailov, D. Grobnic, and C. W. Smelser, "High-temperature multiparameter sensor based on sapphire fiber Bragg gratings," *Opt. Lett.*, vol. 35, no. 16, pp. 2810–2812, 2010.